COMBINED ANALYSIS OF ATMOSPHERIC NEUTRINO RESULTS

G.L. FOGLI, E. LISI, A. MARRONE, and G. SCIOSCIA
Dipartimento di Fisica e INFN, Sezione di Bari
Via Amendola 173, 70126 Bari, Italy

ABSTRACT

The recent observations of atmospheric ν events from the Super-Kamiokande experiment are compatible with two-flavor oscillations in the $\nu_\mu \leftrightarrow \nu_\tau$ channel ("standard" interpretation). Among the possible deviations from this standard picture, we investigate two cases: (1) A specific solution without oscillations (namely, neutrino decay) and (2) Three-flavor oscillations. While the first solution is shown to be incompatible with the data, the second appears perfectly viable, provided that the 3ν oscillations occur dominantly in the $\nu_\mu \leftrightarrow \nu_\tau$ channel and subdominantly in the $\nu_\mu \leftrightarrow \nu_e$ channel. The derivation of such results is based on an updated analysis, including the latest 45 kTy data sample from Super-Kamiokande. A comparison with our previous results, based on 33 kTy data, shows that the oscillation evidence is strengthened, and that the neutrino mass-mixing parameters are constrained in smaller ranges.

1. Introduction

The recent atmospheric neutrino data from the Super-Kamiokande (SK) experiment [1] are in excellent agreement with the hypothesis of flavor oscillations generated by nonzero neutrino mass and mixing [2] in the $\nu_\mu \leftrightarrow \nu_\tau$ channel [3]. Such hypothesis is consistent with all the SK data, including sub-GeV e-like and μ-like events (SG$e, \mu$) [4], multi-GeV e-like and μ-like events (MG$e, \mu$) [5], and upward-going muon events (UPμ) [6], and is also corroborated by independent atmospheric neutrino results from the MACRO [7] and Soudan-2 [8] experiments, as well as by the finalized upward-going muon data sample from the pioneering Kamiokande experiment [9]. Oscillations in the $\nu_\mu \leftrightarrow \nu_\tau$ channel are also compatible with the negative results of the reactor experiment CHOOZ in the $\nu_\mu \leftrightarrow \nu_e$ channel [10].

However, it is important to challenge such "standard interpretation" of the atmospheric neutrino results, by considering departures from the $\nu_\mu \leftrightarrow \nu_\tau$ oscillation dynamics which simply reads:

$$P(\nu_\mu \leftrightarrow \nu_\tau) = \sin^2 2\theta \sin^2 \left(1.27\, m^2\, L/E\right) \ . \tag{1}$$

In the above equation, m^2 is the neutrino square mass difference (in eV^2), L is the neutrino pathlength (in km), and E is the neutrino energy (in GeV).

In this talk we consider two possible departures from the standard $\nu_\mu \leftrightarrow \nu_\tau$ oscillation interpretation. The first case, which is a rather radical alternative, invokes ν_μ decay to explain the SK muon deficit. The second case sticks instead to neutrino

oscillations, but allows other channels to be open through three-flavor oscillations [11]. It will be shown that the first solutions is excluded by the data [12], while the second is perfectly viable. In particular, for the case of 3ν oscillations, we refine previous indications [11] in favor of scenarios with *dominant* $\nu_\mu \leftrightarrow \nu_\tau$ oscillations plus *subdominant* $\nu_\mu \leftrightarrow \nu_e$ oscillations.

Concerning the phenomenological analysis, we use the most recent 45 kTy SK data [13,14]. More precisely, we analyze 30 data points, related to the zenith distributions of sub-GeV events (SG e-like and μ-like, 5+5 bins), multi-GeV events (MGe,μ 5+5 bins) and upward-going muons (UPμ, 10 bins). We also include, when appropriate, the rate of events in the CHOOZ reactor experiment [10] (one bin), which constrains the ν_e disappearance channel. Constraints are obtained through a χ^2 statistic, as described in Ref. [11].

2. SK data and neutrino decay

Neutrino decay has been recently proposed [15] as a possible solution to the atmospheric neutrino anomaly. In a nutshell, the muon neutrino ν_μ is assumed to have an unstable (decaying) component ν_d,

$$\cos\xi \equiv \langle \nu_\mu | \nu_d \rangle \neq 0 \ , \tag{2}$$

with mass and lifetime m_d and τ_d, respectively. In the parameter range of interest, the ν_μ survival probability reads [15]

$$P_{\mu\mu} \simeq \sin^4\xi + \cos^4\xi \exp(-\alpha L/E) \ , \tag{3}$$

where $\alpha = m_d/\tau_d$, and L/E is the ratio between the neutrino pathlength and energy. The possible unstable component of ν_e is experimentally constrained to be very small, so one can take $P_{ee} \simeq 1$.

For large values of $\cos\xi$ and for $\alpha \sim O(D_\oplus/1 \text{ GeV})$ ($D_\oplus = 12,800$ km), the exponential term in Eq. (3) can produce a detectable modulation of the muon-like event distributions [15]. In particular, the expected modulation seems to be roughly in agreement [15] with the reconstructed L/E distribution of contained SK events [3]. However, the L/E distribution is not really suited to quantitative tests, since it is affected by relatively large uncertainties, implicit in backtracing the (unobservable) parent neutrino momentum vector from the (observed) final lepton momentum. Moreover, the L/E distribution includes only a fraction of the data (the fully contained events), and mixes low-energy and high-energy events, making it difficult to judge how the separate data samples (SG, MG, and UP) are fitted by the decay solution.

Therefore, we have tested the neutrino decay hypothesis in a more convincing and quantitative way, by using observable quantities (the zenith distributions of the observed leptons) rather than unobservable, indirect parameters such as L/E.

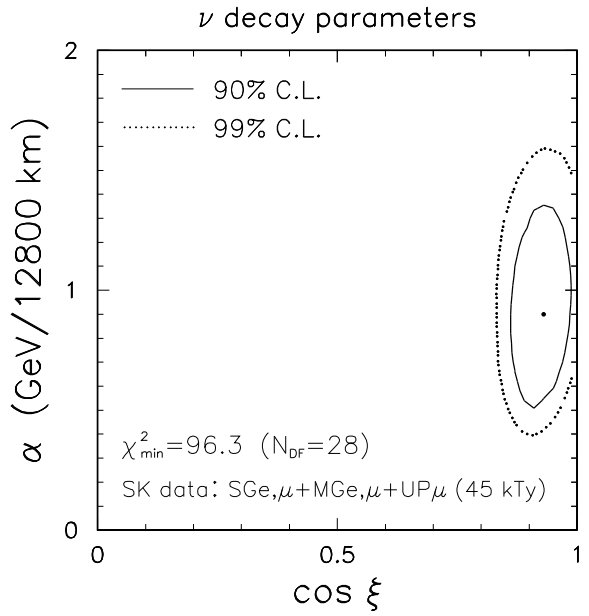

Figure 1: Fit to the Super-Kamiokande data (45 kTy, 30 data points) in the plane of the neutrino decay parameters $\cos\xi = \langle\nu_\mu|\nu_d\rangle$ and $\alpha = m_d/\tau_d$. The solid and dotted lines are defined by $\chi^2 - \chi^2_{\rm min} = 4.61$ and 9.21, corresponding to 90% and 99% C.L. for two variables. The analysis favors $\alpha \sim 1$ GeV$/D_\oplus$ and large $\cos\xi$. However, even at the best fit point there is poor agreement between data and theory ($\chi^2_{\rm min}/N_{\rm DF} = 86.2/28 = 3.1$), indicating that ν decay is not a viable explanation of the Super-Kamiokande observations.

Figure 1 shows the results of our χ^2 analysis in the plane $(\cos\xi, \alpha)$, with α given in unit of GeV$/D_\oplus$. The regions at 90 and 99% C.L. are defined by $\chi^2 - \chi^2_{\rm min} = 4.61$ and 9.21, respectively. As qualitatively expected, the data prefer $\alpha \simeq 1$ and large $\cos\xi$, in order to produce a large suppression of ν_μ's coming from below. However, the absolute χ^2 is always much higher than the number of degrees of freedom, $N_{DF} = 28$ (30 data points $-$ 2 free parameters). In fact, it is $\chi^2_{\rm min} = 86.2$ at the best-fit point [reached for $(\cos\xi, \alpha) = (0.95, 0.90)$]. The very poor global fit indicates that the zenith distributions cannot be accounted for by neutrino decay, contrarily to the claim of [15], which was based on reduced and indirect data (the L/E distribution). This situation should be contrasted with the $\nu_\mu \leftrightarrow \nu_\tau$ oscillation hypothesis, which gives $\chi^2_{\rm min}/N_{\rm DF} \sim 1$ both in two-flavor [3] and three-flavor scenarios (see next section).

Basically, ν decay fails to reproduce the SK zenith distributions for the following reason: The lower the energy, the faster the decay, the stronger the muon deficit — a pattern not supported by the data. This can be better appreciated in Fig. 2, which shows the SK data (45 kTy) and the expectations (at the "best-fit" point) for the five zenith angle (θ) distributions considered in our analysis. In each bin, both the observed and the expected lepton rates R are normalized to the standard values in the absence of decay R_0, so that "no decay" corresponds to $R/R_0 = 1$. The data are shown as dots $\pm 1\sigma$ errors, while the decay predictions are shown as solid lines.

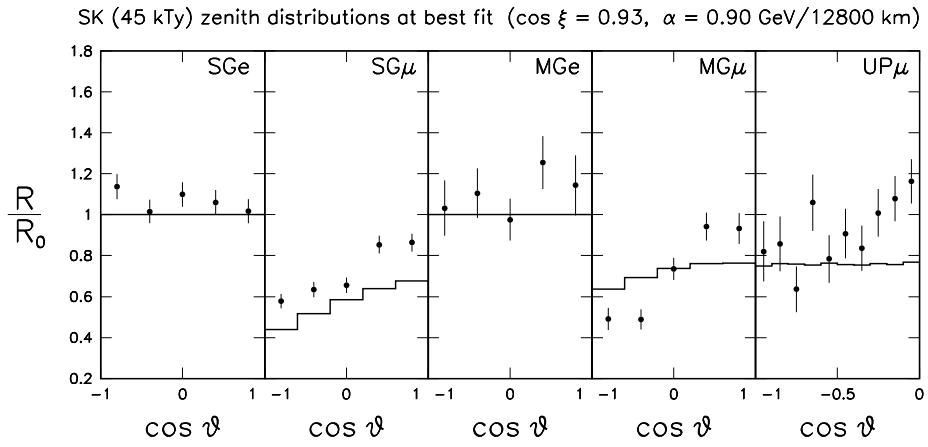

Figure 2: Zenith angle distributions of Super-Kamiokande sub-GeV e-like and μ-like events (SGe and SGμ), multi-GeV e-like and μ-like events (MGe and MGμ), and upward-going muons (UPμ). Data: dots with $\pm 1\sigma$ statistical error bars. Theory (ν decay best fit): solid curves. In each bin, both theoretical and experimental rates R are normalized to their standard (no decay) expectations R_0. The solid curves do not appear to reproduce the muon data pattern.

In Fig. 2, the muon data show significant deviations from the reference baseline $R/R_0 = 1$, most notably for MGμ events. The ν decay predictions also show some (milder) deviations, but their agreement with the data is poor, both in normalization and in shape. Neutrino decay implies a muon deficit decreasing with energy, at variance with the fact that the overall (θ-averaged) deficit is about the same for both SGμ's and MGμ's (-30%). The shape distortions of the muon zenith distributions are also expected to be exponentially weaker at higher energies (i.e., for slower neutrino decay). This makes it impossible to fit at the same time the distorted muon distributions observed at low energy (SGμ) and at high energy (UPμ), and to get a strong up-down asymmetry at intermediate energy (MGμ) as well. Notice in Fig. 2 that, although the predicted *shape* of the zenith distribution appears to be in qualitative agreement with the data pattern for SGμ's, it is not sufficiently up-down asymmetric for MGμ's, and it is definitely too flat for UPμ's, where the muon suppression reaches the plateau $P_{\mu\mu} \simeq c_\xi^4 + s_\xi^4$, in disagreement with the observed $\cos\theta$-modulation.

In conclusion, we have shown quantitatively that the neutrino decay hypothesis, although intriguing, fails to reproduce the zenith angle distributions of the SK sub-GeV, multi-GeV, and upgoing muon data for any value of the decay parameters α and $\cos\xi$. Even at the "best fit" point, data and expectations differ both in total rates and in zenith distribution shapes. Therefore, neutrino decay (at least in its simplest form [15]) is not a viable explanation of the SK observations. The strong disagreement between data and theory was not apparent in [15], presumably because the experimental information used there was rather reduced and indirect.

3. 3ν analysis of SK observations (45 kTy)

While neutrino decay is not a viable explanation of the atmospheric neutrino anomaly, three-flavor oscillations appear to be an appropriate solution with a very rich phenomenology. In this section we mainly present an update of the three-flavor analysis performed in [11], to which we refer the reader for further details. Here we just sketch the method of analysis and the main results using 45 kTY SK data, emphasizing the improvements with respect to the 33 kTy data sample.

The theoretical framework that we adopt for three-flavor oscillations is based on the so-called one mass scale dominance [16], which has been used also for studies of pre-SK atmospheric and reactor neutrino data in Refs. [16,17,18]. In the hypothesis that the two lightest neutrinos (ν_1, ν_2) are effectively degenerate $(m_1^2 \simeq m_2^2)$ (one mass scale dominance), it can be shown [16,11] that atmospheric neutrinos probe only $m^2 \equiv m_3^2 - m_{1,2}^2$, together with mixing matrix elements $U_{\alpha i}$ related to ν_3, namely:

$$\text{Parameter space} \equiv (m^2, U_{e3}^2, U_{\mu 3}^2, U_{\tau 3}^2) \ , \tag{4}$$

where $U_{e3}^2 + U_{\mu 3}^2 + U_{\tau 3}^2 = 1$ for unitarity. The unitarity constraint can be conveniently embedded in a triangle plot [16,17,11], whose corners represent the flavor eigenstates, while the heights projected from any inner point represent the $U_{\alpha 3}^2$'s.

Figure 3 shows the regions favored at 90% and 99% C.L. in the triangle plot, for representative values of m^2. The CHOOZ data, which exclude a large horizontal strip in the triangle, appear to be crucial in constraining three-flavor mixing. Pure $\nu_\mu \leftrightarrow \nu_e$ oscillations (right side of the triangles) are excluded by SK and CHOOZ independently. The center of the lower side, corresponding to pure $\nu_\mu \leftrightarrow \nu_\tau$ oscillations with maximal mixing, is allowed in each triangle both by SK and SK+CHOOZ data. However, deviations from maximal $(\nu_\mu \leftrightarrow \nu_\tau)$ mixing, as well as subdominant mixing with ν_e, are also allowed to some extent. Such deviations from maximal 2ν mixing are slightly more constrained than in the previous analysis of the 33 kTy SK data [11].

Figure 4 shows the constraints on the mass parameter m^2 for unconstrained three-flavor mixing. The best fit value is reached at $m^2 \sim 3 \times 10^{-3}$ eV^2, and is only slightly influenced by the inclusion of CHOOZ data. However, the upper bound on m^2 is significantly improved by including CHOOZ. As compared with the corresponding plot in Ref. [11] (33 kTy), this figure shows that the 45 kTy data are in better agreement with the oscillation hypothesis (lower χ^2). Moreover, the favored range of m^2 is restricted by $\sim 10\%$ with respect to Ref. [11].

Figures 3 and 4 clearly show the tremendous impact of the SK experiment in constraining the neutrino oscillation parameter space. Prior to SK, the data could not significantly favor $\nu_\mu \leftrightarrow \nu_\tau$ over $\nu_\mu \leftrightarrow \nu_e$ oscillations, and could only put weak bounds on m^2 (see Refs. [17,18]). In addition, Figure 4 shows that the neutrino oscillation hypothesis is in excellent agreement with the data (as opposed to the neutrino decay hypothesis examined in the previous section).

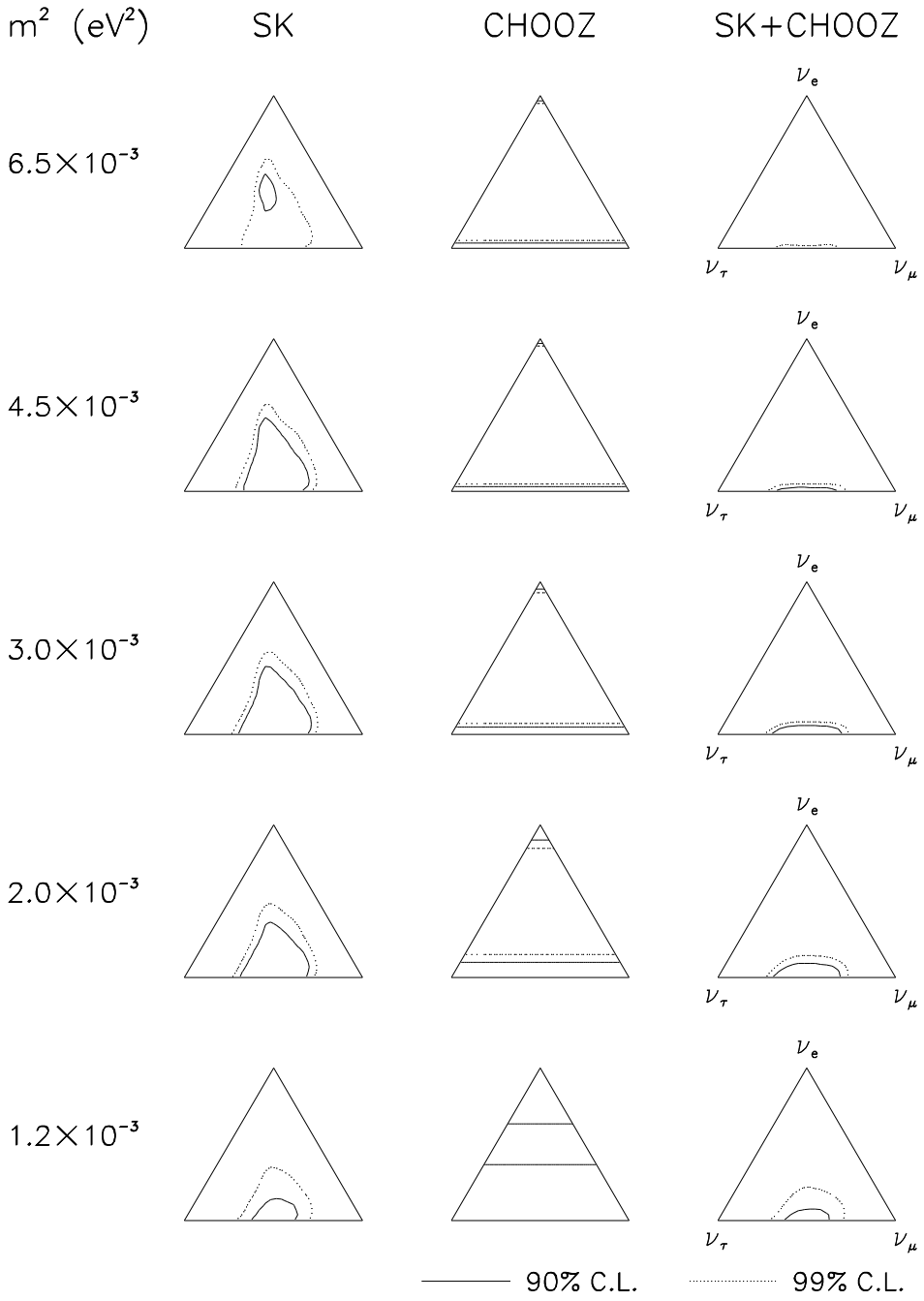

Figure 3: Three-flavor analysis in the triangle plot, for five representative values of m^2. Left and middle column: separate analyses of Super-Kamiokande (45 kTy) and CHOOZ data, respectively. Right column: combined SK+CHOOZ allowed regions. Although the SK+CHOOZ solutions are close to pure $\nu_\mu \leftrightarrow \nu_\tau$ oscillations, the allowed values of U^2_{e3} are never negligible, especially in the lower range of m^2.

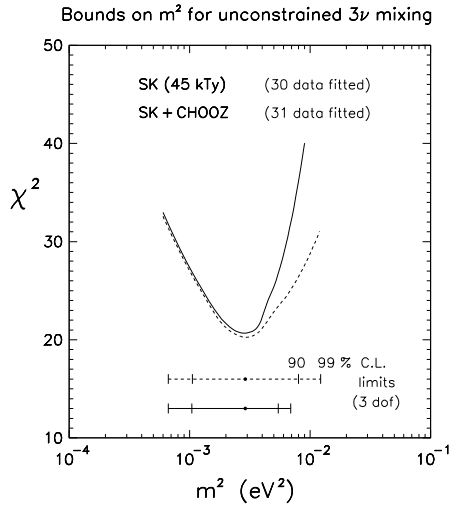

Figure 4: Values of χ^2 as a function of m^2, for unconstrained three-flavor mixing. Dashed curve: fit to SK data only (45 kTy). Solid curve: fit to SK+CHOOZ. The minimum of χ^2 is reached for $m^2 \simeq 2.8 \times 10^{-3}$ eV^2.

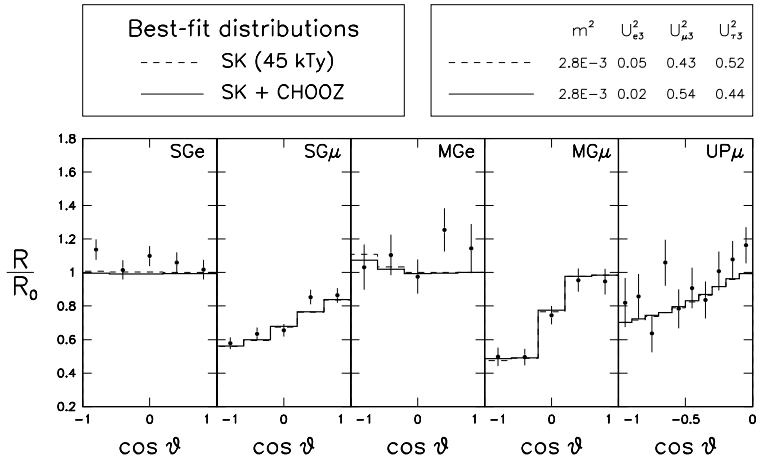

Figure 5: SK zenith distributions of leptons at best fit (dashed lines), also including CHOOZ (solid lines), as compared with the 45 kTy experimental data (dots with error bars). The 3ν mass-mixing values at best fit are indicated in the upper right corner. The theory/data agreement is excellent.

Finally, Fig. 5 shows the best-fit zenith distributions of SG$e, \mu$, MG$e, \mu$, and UPμ events, normalized to the no-oscillation rates in each bin. There is excellent agreement between data and theory, especially for the μ distributions. The nonzero value of U^2_{e3} at best fit leads to a slight expected electron excess in the MGe sample for $\cos\theta \to -1$. The observed electron excess is, however, somewhat larger than expected, both for SGe's and for MGe's. A significant reduction of the statistical error is needed to probe possible MGe distortions, which would be unmistakable signals of subdominant $\nu_\mu \to \nu_e$ oscillations.

4. Conclusions

The recent Super-Kamiokande data are sufficiently precise to test explanations beyond standard $\nu_\mu \leftrightarrow \nu_\tau$ oscillations. In particular, they exclude neutrino decay (at least in its simplest version), and are instead consistent with three-flavor oscillations dominated by $\nu_\mu \leftrightarrow \nu_\tau$ transitions. The amplitude of the $\nu_\mu \leftrightarrow \nu_e$ channel is not necessarily zero, although being strongly constrained by both SK and CHOOZ. A contribution from the $\nu_\mu \leftrightarrow \nu_e$ channel might explain part of the electron excess observed in SK, especially for multi-GeV e-like events. Higher statistics is needed to test such interpretation. Increasingly strong indications are seen to emerge in favor of the oscillation hypothesis, and against more exotic scenarios such as neutrino decay.

Acknowledgments. G.L.F. thanks Milla Baldo Ceolin for kind hospitality.

5. References

1) K. Scholberg, these Proceedings.
2) B. Pontecorvo, Sov. Phys. JETP **26**, 984 (1968).
3) SK Collaboration, Y. Fukuda *et al.*, Phys. Rev. Lett. **81**, 1562 (1998).
4) SK Collaboration, Y. Fukuda *et al.*, Phys. Lett. B **433**, 9 (1998).
5) SK Collaboration, Y. Fukuda *et al.*, Phys. Lett. B **436**, 33 (1998).
6) SK Collaboration, Y. Fukuda *et al.*, Phys. Rev. Lett. **82**, 2644 (1999).
7) MACRO Collab., M. Ambrosio *et al.*, Phys. Lett. B **434**, 451 (1998).
8) Soudan-2 Collab., W.W.M. Allison *et al.*, Phys. Lett. B **449**, 137 (1999).
9) Kamiokande Collaboration, Phys. Rev. Lett. **81**, 2016 (1998).
10) CHOOZ Collab., M. Apollonio *et al.*, Phys. Lett. **B** 420, 397 (1998).
11) G.L. Fogli, E. Lisi, A. Marrone, and G. Scioscia, Phys. Rev. D **59**, 033001 (1999).
12) G.L. Fogli, E. Lisi, A. Marrone, and G. Scioscia, Phys. Rev. D **59**, 117303 (1999).
13) M. Messier, in *DPF'99*, Proceedings of the 1999 Meeting of the American Physical Society, Division of Particles and Fields, to appear. Transparencies available at http://www.physics.ucla.edu/dpf99 .
14) A. Habig, in *DPF'99* [13], hep-ex/9903047.
15) V. Barger, J.G. Learned, S. Pakvasa, and T.J. Weiler, Phys. Rev. Lett. **82**, 2640 (1999); see also S. Pakvasa, these Proceedings.
16) G.L. Fogli, E. Lisi, and G. Scioscia, Phys. Rev. D **52**, 5334 (1995).
17) G.L. Fogli, E. Lisi, D. Montanino, and G. Scioscia, Phys. Rev. D **55**, 4385 (1997).
18) G.L. Fogli, E. Lisi, and A. Marrone, Phys. Rev. D **57**, 5893 (1998).